SINTEF
PROCEEDINGS
4

Selected papers from the 10th Trondheim Conference on CO_2 Capture, Transport and Storage

TCCS-10

SINTEF Proceedings

Editors:
Nils A. Røkke and Hanna Knuutila

TCCS–10
CO_2 Capture, Transport and Storage
Trondheim 17th–19th June 2019

Selected papers

SINTEF Academic Press

SINTEF Proceedings no 4
Editors: Nils A. Røkke (SINTEF) and Hanna Knuutila (NTNU)
TCCS–10
CO_2 Capture, Transport and Storage. Trondheim 17th–19th June 2019
Selected papers from the 10th International Trondheim CCS Conference

Keywords:
CCS – Carbon Capture, Transport and Storage, CO_2 Capture, CO_2 Transport, CO_2 Storage, CO_2 Utilization, Pre-combustion capture, Post-combustion capture, Oxy-fuel capture, CCS and hydrogen, CO_2 positive solutions, International R&D activities, Whole system issues, Novel CCS technologies, Public Acceptance, Communication, Policy, Business models

Cover illustration: SINTEF Energy

ISSN 2387-4295 (online)
ISBN 978-82-536-1646-9 (pdf)

SINTEF Academic Press
Address: Børrestuveien 3
PO Box 124 Blindern
N-0314 OSLO
Tel: +47 40 00 51 00

www.sintef.no/community
www.sintefbok.no

SINTEF Proceedings
SINTEF Proceedings is a serial publication for peer-reviewed conference proceedings on a variety of scientific topics.
The processes of peer-reviewing of papers published in SINTEF Proceedings are administered by the conference organizers and proceedings editors. Detailed procedures will vary according to custom and practice in each scientific community.

DEVELOPMENT OF SILICA SODALITE WITH ENHANCED POROSITY VIA TOPOTACTIC SYNTHESIS FOR PRE COMBUSTION CO_2 CAPTURE

C-I. Eden, N. Ntombela, M.O. Daramola*

School of Chemical and Metallurgical Engineering, Faculty of Engineering and the Built Environment, University of the Witwatersrand, Johannesburg, South Africa

* Corresponding author e-mail: michael.daramola@wits.ac.za

Abstract

Topotactic conversion of layered silicates is reported to yield sodalite with enhanced frameworks, chemical compositions and predictable outcomes. Traditional hydrothermal synthesis results in sodalite with occluded matter preventing the effective use of sodalite cages for adsorption and separation applications. However, the reproducibility of high quality silica sodalite depends on obtaining optimized synthesis conditions and investigating the effect these conditions is essential. A 2^3 factorial design was employed to investigate the effect of process variables (acid strength, acid treatment time and calcination temperature) on the quality of silica sodalite produced via topotactic conversion in this study. XRD, SEM and Nitrogen physisorption at 77K were used for physio-chemical characterization of the sodalite samples. The produced sodalite crystals were used in membrane synthesis, and the membrane was tested for $CO_2/H_2/N_2$ separation. Sodalite of desirable crystallinity and plate-like morphology was produced with surface area and porosity of 79.44m^2/g and 0.081cm^3/g, respectively. An incomplete transformation of sodalite at low acid concentration and treatment time was experienced. A significant improvement on surface area and pore volume was reported on all samples as compared to that of the hydroxy sodalite. Analysis of the regression model obtained from the experimental data indicates acid treatment time as an insignificant variable. The preliminary investigation of the application for membrane synthesis indicates enhanced porosity of the HSOD improved the membrane H_2 permeance by 178%.

Keywords: *Silica sodalite, Topotactic conversion, Response surface methodology*

1. Introduction

Increasing levels of anthropogenic CO_2 have been noted as a major cause for environmental climate change. The most effective means for remediation focuses on point-source emission such as power plants [1]. The majority of the world's energy production comes from the combustion of fossil fuels, and an example of a system employed to achieve this is the Natural Gas Combined Cycle (NGCC) or Integrated Gasification Combined Cycle (IGCC) which result in large volumes of CO_2 emissions [2]. The depletion of fossil fuels and the increasing energy demand have led to a global movement towards high energy efficiency of industrial processes and the capture of point-source CO_2 emissions [3, 4]. Carbon capture from power generation is possible through three ways; pre-combustion, post combustion and oxy-fuel combustion capture. Pre-combustion carbon capture is typically favoured in coal burning IGCC power generation due to the high concentration of CO_2 in the flue gas (>20%) which improves the sorption efficiency and increases the heating value of the hydrogen fuel stream [5, 6]. For these reason a large amount of research has gone into the separation of CO_2 from gases such as H_2 and CH_4.

Traditional large scale CO_2 separation methods such as pressure-swing adsorption and cryogenic distillation are preferred due to their reliable nature, superior separation and low capital costs but are highly energy intensive and utilize environmentally damaging chemicals [7, 8]. Membrane systems provide an alternative with low energy intensity, operating and capital costs as well as high flux [9]. However, the high temperature and steam utilized in coal gasification means that membranes used for in pre-combustion CO_2 capture need to be thermally and hydro-thermally stable, with good separation performance to make them an economically feasible alternative to traditional methods [9, 10]. Polymeric membranes form the majority of membranes current used in industry, however these membranes can be brittle and exhibit an undesirable trade-off between permeability and selectivity [7]. Mixed matrix membranes (MMM) combine the high selectivity and easily processable nature of polymers with inorganic materials such as zeolites, and are being intensively investigated for gas separations [1, 11-13]. One candidate material employed in membrane development and applicable in pre-combustion CO_2 capture is hydroxy sodalite [14, 13].

Hydroxy sodalite is a common zeolite with cage structures consisting of 4 and 6 ring sodalite cages with pores of approximately 2.2 Å [15-17]. Sodalite has shown promise in membrane applications due to its low framework density and small cage apertures (0.265 nm) which could effectively separate small atoms such as hydrogen (0.289 nm) from carbon dioxide (0.33 nm) [12, 13]. Synthetic sodalite fabricated via the hydrothermal method typically contain less occluded water but large

volumes of occluded organic matter from solvents and structure directing agents (SDA) used during synthesis as well as small molecules such as hydrogen and helium which block pores and prevent the effective use of the sodalite cages [9, 14]. Removing these occluded materials from the cage via dehydration or calcination at high temperatures (> 450°C) collapses the cage, rendering the sodalite ineffective [14, 18, 19]

Topotactic conversion is a relatively new synthesis method that enables the production of zeolite structures with unique new chemical frameworks, compositions and morphologies [20]. In the past decade a number of zeolites have been successfully fabricated from layered silicates using the topotactic conversion process, some of these include MWW, RUB-24 and RUB-41 [21, 22]. Sodalite formed through this method report the absence of occluded matter and increased porosity [15].

Moteki et al. [15] noted that that acid treatment with small carboxylic acids would shorten the interlayer distance and translate the layers in a parallel direction to facilitate guest exchange and produce pure silica sodalite. However, the samples produced after calcination were amorphous. This was attributed to differences in the interlayer environments caused by the gradual elimination of organic guest species. Moteki et al [19] went on to further understand the conversion process by investigating the effect of the length of the alkyl chain, the strength of the acid and the acid treatment time. Good crystallinity was observed for samples treated with acetic or propionic acid in concentrations from 3 to 9 M, with samples treated with propionic acid displaying the highest crystallinity. While those treated with formic or butyric acid resulted in amorphous products after calcination. The use of 1M propionic acid resulted in low crystallinity which was attributed to poor ion exchange and non-uniform interlayer distances. The crystallinity of the samples increased with increasing acid treatment time from 10 seconds to 10 minutes, no further improvements for samples treated up to 3 hours were recorded but residual TMA+ cations were noted in samples treated for less than 3 hours. In spite of inconsistencies in the results, Moteki and his associates concluded that effective synthesis of pure silica sodalite through topotactic conversion is realizable [19].

Koike et al. [20] proposed a stepwise method including intercalation of N-methylformamide (NMF) into the acid treated RUB-15 before calcination for the synthesis of silica sodalite. Furthermore, the authors use both HCl and acetic acid to treat the RUB-15. All samples prepared using HCl were reported to be amorphous after calcination while plate-like sodalite was successfully synthesized with acetic acid (6M). In addition, the role of the NMF was suggested to be similar to that of the SDA, but yielded an inferior quality of sodalite to those produced hydrothermally.

Evidently, previous studies have shown inconsistencies in the synthesis of silica sodalite produced via topotactic conversion thereby diminishing its reproducibility. Furthermore, the influence of synthesis conditions is shown to be a major hurdle. In depth understanding of the influence of synthesis conditions would be paramount to developing a robust technique for the reproducible synthesis of silica sodalite via topotactic conversion. This study investigated the effect of synthesis conditions on the textural and morphological quality of silica sodalite produced in order to optimize the pore volume of the synthesized sodalite. A preliminary investigation on the application of the produced crystals in membrane synthesis and application was carried out as well.

2. Experimental

2.1 Materials

Tetra-ethoxysilane (TEOS, reagent grade 98%, Sigma-Aldrich, South Africa), tetrametyl ammonium hydroxide (TMAOH, 25wt.% in water, Sigma-Aldrich, South Africa) and acetone (Sigma-Aldrich, South Africa) were used for the synthesis of RUB-15. Propionic acid (>99.5wt.%, Sigma-Aldrich, South Africa) was used for the acid treatment of RUB-15 in the synthesis of silica sodalite. Sodium metasilicate (Sigma-Aldrich, South Africa), sodium hydroxide pellets (Sigma-Aldrich, South Africa) and anhydrous sodium aluminate (Sigma-Aldrich, South Africa) was used for the production of hydroxy sodalite (HSOD) for comparison. Membranes were prepared from polysulfone (PSf, beads (transparent), Sigma-Aldrich, South Africa) and N,N-Dimethylacetamide (>99.9%, Sigma-Aldrich, South Africa). Pure gas cylinders were purchased from Afrox, South Africa (N_2, H_2, CO_2, >99.9%).

2.2 Synthesis methods

The procedure stipulated by Moteki et al. was used for the synthesis of RUB-15 [19]. TEOS and TMAOH were combined in a 1:1 molar ratio and stirred for 24 hours to homogenize. The solution was then placed in a Teflon autoclave and heated at 413 K for 7 days. RUB-15 was recovered as a white waxy substance, which was washed with acetone, separated by centrifugation and dried overnight at 333 K in a convection oven to yield a white powder.

The obtained RUB-15 (0.1 g) was dispersed in propionic acid (30 ml) of varying concentrations (1-5 M) and stirred at 900 rpm for various time periods (10-180 minutes). The solution was separated by centrifugation, washed repeatedly with deionized water and dried in a convection oven overnight at 333 K. The samples were then calcined for 5 hours at temperatures between 1073 and 1173 K.

HSOD crystals were synthesized by hydrothermal synthesis using sodium metasilicate, sodium hydroxide pellets, anhydrous sodium aluminate, and deionized water as described by Daramola et al. [14].

2.3 Characterization of synthesized particles

Powder X-ray diffraction (XRD) patterns were performed on both the precursor RUB-15 layers as well as the calcined sodalite using a Bruker D2 XRD with CuKα radiation (λ = 1.54060 Å) to analyze the crystalline and amorphous nature of the sodalite. Scanning electron microscopy (SEM) was conducted on a Carl Zeiss sigma field emission scanning electron microscope equipped with Oxford X-act EDS detector to examine the surface morphology and elemental composition of the samples.

Single point Brunauer-Emmett-Teller (BET) analysis was conducted from the results of Nitrogen Physisorption at 77 K, to determine the surface area (SA) and pore volume (PV) and pore size (PS) of the sodalite samples.

2.4 Experimental design

A statistical approach using response surface methodology was employed to investigate the effect of synthesis variables on sodalite quality. A 2^3 full factorial design was utilized to reduce the number of experimental runs as opposed to traditional design methods as well as to account for the main and interactive effects of the variables. Design Expert v.11 Software (Stat-Ease, USA, 2018) and Matlab software (2016) was used to statistically analyse the experimental data. The 2^3 factorial design was implemented to investigate 3 factors at 2 levels producing a minimum of 8 runs. Three factors were considered; acid concentration (A), acid treatment time (B) and calcination temperature (C). The 2 levels and the mid-level (also referred to as the center point) utilized for each factor as tabulated in the experimental design scheme (Table 1).

Table 1: Experimental Design Scheme

Run	Coded Values			Actual values		
	A	B	C	A	B	C
	M	minutes	K	M	minutes	K
SSOD 1	1	1	-1	5	180	1073
SSOD 2	-1	1	-1	1	180	1073
SSOD 3	1	-1	-1	5	10	1073
SSOD 4	-1	-1	-1	1	10	1073
SSOD 5	1	1	1	5	180	1173
SSOD 6	-1	1	1	1	180	1173
SSOD 7	1	-1	1	5	10	1173
SSOD 8	-1	-1	1	1	10	1173
SSOD 9	0	0	0	3	95	1123

A) Acid concentration; B) Acid treatment time; C) Calcination temperature

The center point was included in the study to improve statistical significance and aid in exploring the curvature effect in the design space [23]. Due to limited resources a single replicate was utilized preventing the estimation of pure error. It was assumed that the system was dominated by the main effects and low-order interactions, following the effect sparsity principle [24].

2.5. Model Formulation

A general regression model was assumed (Equation 1) and the experimental data was utilized to determine the best model. Design Expert v.11 Software (Stat-Ease, USA, 2018) and Matlab Software (2016) were used to investigate ten candidate models.

$$y = \beta_0 + \beta_a A + \beta_b B + \beta_c C + \beta_{ab} AB + \beta_{bc} BC + \beta_{ac} AC + \beta_{abc} ABC \pm \epsilon \quad \text{Equation 1}$$

In Equation 1, y represents the system response (pore volume), β_o the intercept of the regression line, $\beta_{a,b,c}$ the regression coefficients for the respective synthesis variables A (acid concentration), B (acid treatment time) and C (calcination temperature), with ϵ being the mean square error.

An ANOVA test was performed on each candidate model and the P values (within 95% confidence interval) for each model term and the model as a whole was assessed to determine significance. Lacks of fit tests of the suggested model were also calculated within a 95% confidence interval, the coefficient of determination (R^2), the adjusted R^2 as well as the mean square error were evaluated to produce the suggested model.

2.6. Membrane synthesis and single gas permeation tests

Membrane synthesis followed the phase inversion technique as documented elsehwere [18]. To fabricate the membranes, individual measurements of SSOD (0 and 5 wt. %) as well as HSOD (5 wt. %) were mixed with 20 ml of N,N Dimethylacetamide for 3 hours before 5 g polysulfone was added and stirred for a further 24 hours. The mixture solution was repeatedly ulltra-sonicated and mixed to ensure a homogeneous mixture. The solution was cast into a thin film membrane using a "doctor" blade and a glass plate. Membranes were immediately submerged in deionized water and soaked for 24 hours. The membranes were then oven dried at 333 K for 2 hours. Membrane thickness (l) was measured using a digital outside micrometre (InSize, 3109-25A).

The single gas permeation tests were carried out using pure component of N_2, H_2, and CO_2 in a custom-built separation rig using a membrane area (A) of 9.6 cm^2. The feed upstream pressure was set to 1 bar_g at ambient conditions (temperature = 298K). The pure gas permeability (P) was calculated following Equation 2 in Barrer (1 Barrer = 1×10^{-10} cm^3(SPT).cm/cm^2.s.cmHg) [9, 12]. The volumetric gas flowrate (Q) and transmembrane pressure (Δp) were measured from the rig. Dividing permeability by membrane thickness yields the membrane permeance. Measurements were converted to SI units
(1 Barrer = 3.35×10^{-16} mol.m/m^2.s.Pa).

$$P = \frac{l\,Q}{A\,\Delta p}\,\frac{273.15}{T} \quad \text{Equation 2}$$

From the individual permeability, the ideal selectivity (α) for gas A over gas B was calculated using Equation 3.

$$\alpha_{A/B} = \frac{P_A}{P_B} \quad \text{Equation 3}$$

3. Results and discussion

3.1. Physio-chemical characterization

3.1.1. Crystallinity and morphology

The RUB-15 synthesized displayed some of the characteristic peaks shown in literature such as the peaks at 2θ= 15° and 22° (Figure 1) [25, 26, 15]. However, the strongest characteristic peak at 2θ = 6.3° is not present in the XRD pattern. A significant amount of noise is present and the low crystallinity suggests a high volume of intercalated TMA^+ cations [19]. The SEM images of the RUB-15 depict the plate-like morphology of similarly sized and shaped plates, superposed onto one another in agreement with Moteki et al [19].

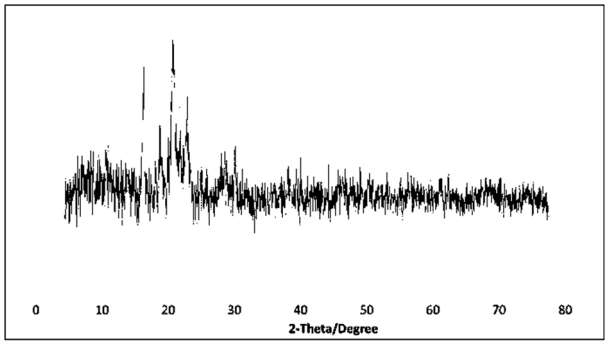

Figure 1: XRD pattern for synthesized RUB-15.

The HSOD synthesized hydrothermally for comparison shows correctly positioned XRD diffraction peaks and good crystallinity (Figure 2) in line with the work conducted by Daramola, et al and the IZA simulated octahydrate standard [14, 27]. In comparison to the sodalite synthesized via topotactic conversion the HSOD displays higher crystallinity and a greater number of the characteristic peaks.

The samples prepared from the propionic acid treatment and calcination of synthesized RUB-15 displayed XRD patterns (Figure 2) with two of the characteristic peaks of the IZA SOD standard, specifically at 2θ= 12.2° and 21.2° [27]. All of the samples display a large volume of noise and an amorphous hump indicating incomplete transformation of the crystalline phase due to the formation of intra-layer Si-O-Si bridges [28]. Considering the poor crystallinity of the synthesized RUB-15 precursor, poor crystallinity is expected in the produced sodalite samples. Silica sodalite sample 4 (SSOD4) was initially dominated by noise and impurities (as seen by the background pattern) but when repeated displayed the significant peaks at low intensities and a smooth pattern as shown in Figure 2. This clearly highlights an inconsistency in reproducibility. The intensity of diffraction peaks was seen to decrease with increasing sample number and a tradeoff between the second peak (2θ = 21.2°) and hump intensity was evident in the remaining samples. This may be attributed to incorrect layer translation with lower acid strength and treatment time [15].

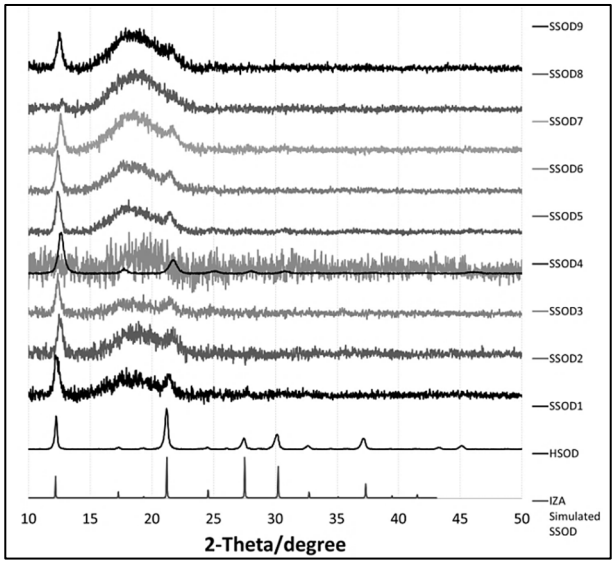

Figure 2: XRD pattern for sodalite samples (SSOD Run 1-9, RUB-15, HSOD and the IZA simulated sodalite standard)

SEM images of the synthesized HSOD show spherical morphology consisting of agglomerated rod-like structures (Figure 3b). SSOD2 and SSOD3 were determined to be of the closest morphology to RUB-15 (Figure 3c and 3d), showing plate-like morphology of larger, irregular sized plates with curled edges superposed on one another. This is similar but not identical to that of RUB-15 which depicts the layering of smaller plates (Figure 3a). This is attributed to inconsistencies in the thickness of the plates resulting in thinner plates becoming more wrinkled and curled during the condensation process [28]. SEM imaging on SSOD 4-9 produced a plate like morphology and varying degrees of curling which can be seen in the supplementary data.

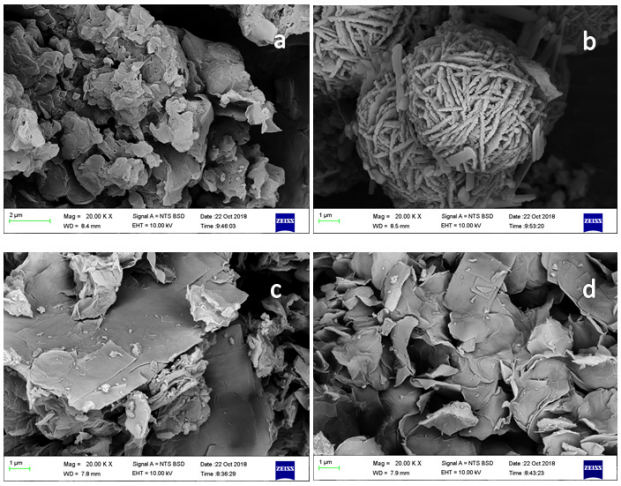

Figure 3: SEM imagines of a) RUB-15; b) HSOD; c) SSOD2; d) SSOD3

3.1.2. Textural properties

The pore volume produced from Brunauer-Emmett-Teller (BET) analysis results were used as the model response [29]; the determined model was then utilized to define optimum synthesis parameters in order to maximize the response.

HSOD was synthesized to form a baseline for comparing the sodalite surface area and pore volume. The HSOD surface area (SA) and pore volume (PV) were 2.35m^2/g and 0.012cm^3/g, respectively. SSOD 2 displayed the highest surface area and pore volume, with suitable XRD results and SEM images. Moteki and associates [19] concluded that at low acid concentrations poor crystallinity was produced, presumably due to a low degree of ion exchange, yet in this study SSOD2 synthesized at low acid concentration, low acid treatment time and low calcination temperature yielded the greatest surface area and pore volume. BET results for SSOD2 yielded a surface area and pore volume of 79.44m^2/g and 0.081cm^3/g, respectively. All samples showed increased surface area and pore volume with decreased pore size, relative to HSOD (Table 3). SSOD 2 and 3 were identified to be of the best quality despite conflicting acid concentrations.

Significant reductions in pore size of the synthesized sodalite nanoparticles as compared to hydroxy sodalite

were also observed. The synthesized silica sodalite nanoparticles are characterized as mesoporous with pore diameters between 2-50 nm. The small porosity could be instrumental to separating small molecules such as H_2 H_2O and NH_3 from bigger molecules.

Table 2: BET results for synthesized samples

Run	BET Results			Relative to HSOD		
	SA	*PV*	*PS*	*SA*	*PV*	*PS*
	m^2/g	cm^3/g	*nm*	m^2/g	cm^3/g	*nm*
SSOD1	42.91	0.065	6.09	18.29	5.49	0.30
SSOD2	79.44	0.081	4.08	33.87	6.81	0.20
SSOD3	70.54	0.072	4.07	30.07	6.03	0.20
SSOD4	43.61	0.064	5.87	18.59	5.37	0.29
SSOD5	18.85	0.046	9.81	8.04	3.89	0.48
SSOD6	26.02	0.052	7.96	11.09	4.35	0.39
SSOD7	23.38	0.051	8.76	9.97	4.30	0.43
SSOD8	42.27	0.064	6.06	18.02	5.38	0.30
SSOD9	21.74	0.049	8.97	9.27	4.10	0.44
HSOD	2.35	0.012	20.29	1.00	1.00	1.00

3.2. Pore volume regression model

Response surface methodology was utilized to better understand the main and interactive effects of the topotactic synthesis variables on the porosity of the sodalite produced. The half-normal (Figure 4a) and Pareto Plots (Figure 4b) were evaluated to determine the significant factors. Factor C- temperature and Factor A- acid concentration fall to the right of the half-normal plot and were recommended as key factors. Factor C- temperature has a much greater standardized effect and this can be seen in the Pareto plot where only factor C- temperature is likely to be a significant model term.

Multiple candidate models (linear, 2 and 3 factor interaction, quadratic) were examined for the best fit to experimental data using regression analysis. The majority of these models produced good regression coefficients but high P values leading to an insignificant model. In all candidate models factor B- acid treatment time had an exceptionally high P value and was determined to have close to no effect on the response, for this reason it was removed from the model equation and should not be considered a critical synthesis parameter for future work. This result is corroborated by the report of Moteki et al, where no difference in sodalite crystallinity for samples treated for 10 minutes as opposed to those treated for 3 hours was reported [19].

A model utilizing factors A and C was adopted as the best fit to experimental data, displaying high regression with sufficiently low p-value. The empirical model suggested to relate synthesis variables to pore volume is expressed in Equation 4.

$$PV = 0.2599 - 1.64X10^{-3}A - 1.72X10^{-4}C \pm 2.98X10^{-5}$$

Equation 4

ANOVA analysis of the suggested model revealed a significant model of a sufficiently low probability value of 0.0428 (P <0.05) within a 95% confidence interval. While good correlation between the experimental values and the regression model as stated by the coefficient of determination (R^2) of 0.7164 was observed, this value is not as close to 1 as desired. This indicates 28.36% of the total variation was unexplained by the suggested model as can be seen from the spread of points from the regression line on the graph of experimental and predicted values in Figure 4c.The greater the F value for each term, the greater the effect that variable will have on the response [30].

Factor C was concluded to be a significant model term with a p-value of 0.021 ($p < 0.0500$) and F value of 8.4 indicating a significant contribution to the response. An adequate precision value of 5.127 was calculated. This represents the signal to noise ratio. As the value is above 4, the signal was determined to be of adequate strength to navigate the design space (Table 4). A low coefficient of variance (C.V. %) indicates the good reliability and high precision in the suggested model, the calculated value of 12.12 % shows adequate reliability and precision. The graph of internally studentized residuals (Figure 4d) confirms the independence assumption and exhibits random scatter. All points fall within the limits and the absence of clustered data confirms satisfactory fit of the proposed model.

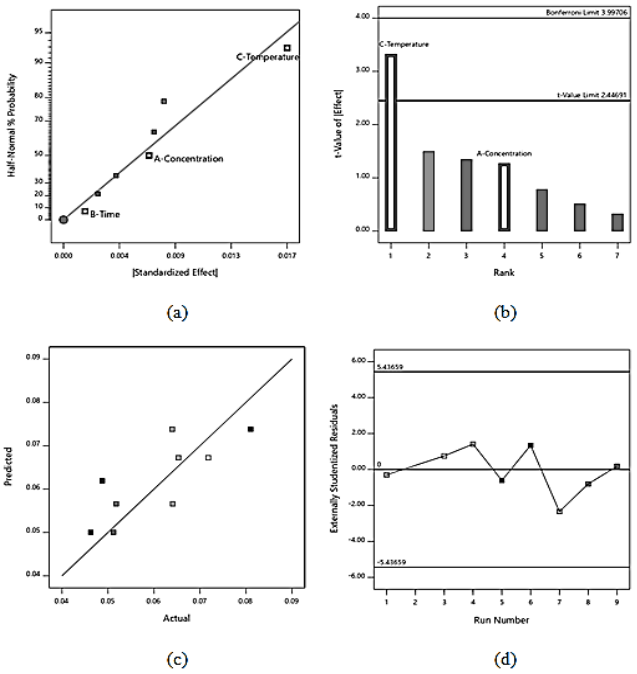

Figure 4: a) Half-normal; b) Pareto chart; c) Predicted versus actual values; d) Residual versus run plot

Table 3: Analysis of variance for main effects of the variables

Source	Sum of squares	df	Mean	F-value	p-value
Model	67.8×105	2	33.9×105	6.315	0.043
A	8.63×105	1	8.63×105	1.609	0.261
C	59.1×105	1	59.1×105	11.020	0.021
Curvature	0.000154	1	1.54×105	2.8687	0.151
Residual	0.000268	5	5.36×105		

Cor Total	0.0011	8			

Table 4: Statistical parameters

Std. Dev.	0.007	R^2	0.716
Mean	0.060	Adjusted R^2	0.603
C.V. %	12.115	Adeq Precision	5.128

The 3-D response surfaces and 2-D Contours visually describe the effects of the independent variables and their interactions on the response. The curvature of the system was found to be insignificant in the ANOVA analysis however, removing this term renders the model insignificant. The lack of curvature in the design space can be seen by the straight contour lines in Figure 5b. Lower acid strength and lower calcination temperature can be seen to produce greater pore volume of the nanoparticles. It could be speculated that lower acid strength correlates to a lower degree of ion exchange and the inhibition of well-ordered silicate layers, thereby resulting in poor crystallinity [19]. Thus it could be explained that the high surface area and pore volume produced is as a result of high degree of ion exchange between interlayer TMA^+ and H^+ cations leading to the rapid formation of Si-OH bonds with greater removal of TMA^+ cations, resulting in enhanced cage dimensions [19]. Lower calcination temperature is favourable for increased porosity as decomposition of interlayer propionic acid is limited (>873 K). Complete removal of organic matter at higher temperatures through the small sodalite cage aperture could result in the collapse of the cage structures and reduced porosity [31].

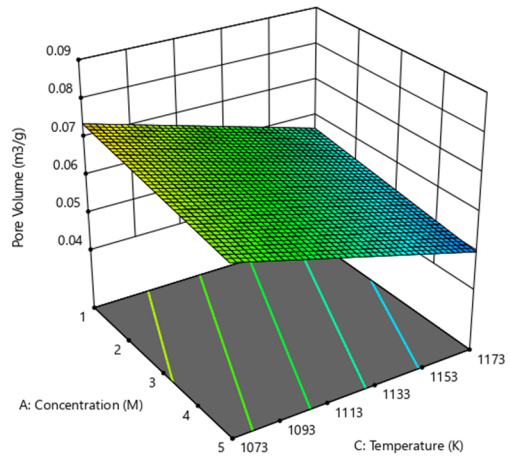

(a)

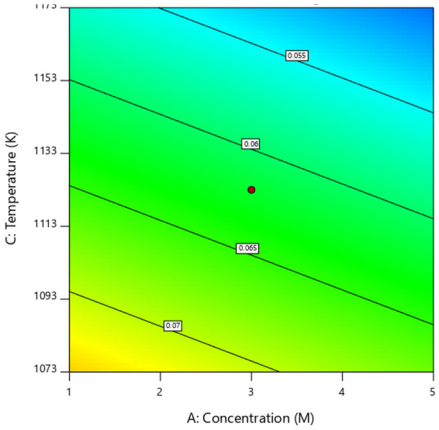

(b)

Figure 5: (a) 3-D response surface and (b) 2-D contour diagram showing the interaction between acid strength (A) and calcination temperature (C) at (B = 95 min)

3.3. Model validation

Synthesis variables were tested for reproducibility and model confirmation (Table 5). New RUB-15 was synthesized following the same procedure and found to have a higher crystallinity than that initially reported in this study. While this facilitated greater crystallinity in the product, the pore volume of the produced sodalite samples exhibited a large error in relation to the model predicted values. This highlights problems with reproducibility of the process and the modeling of synthesis factors due to the 2-stage synthesis; synthesis of RUB-15 and conversion to SSOD.

Table 5: Model validation

A	B	C	Experimental (cm^3/g)	Predicted (cm^3/g)	Error (%)
1	180	1173	0.043	0.057	32.56
5	180	1173	0.061	0.050	18.03

Optimization was conducted maximizing surface area and pore volume and minimize pore size while keeping the synthesis parameters within the upper and lower limits. An optimal surface area, pore volume and pore size of 56.72 m^2/g, 0.074 cm^3/g and 0.5026 nm respectively were proposed at 1M, 95 minutes and 1073 K. Low calcination temperatures were desirable to maximize both surface area and pore volume.

4. Membrane synthesis and single gas permeation tests

A preliminary study was conducted to investigate the synthesis and performance of mixed matrix membrane obtained using the SSOD (SSOD infused PSf membranes). The synthesized SSOD (5 wt. %) and HSOD (5 wt. %) were infused into polysulfone (PSf) and tested for the separation of H_2/CO_2. These membranes displayed an asymmetric morphology common to polysulfone (SEM images are not shown in this article) [32, 18]. Results of single gas permeation reveal that addition of SSOD with enhanced porosity displayed H_2 permeance of 178% higher than that of a PSf membrane infused with HSOD (see Table 6). This permeance is in

slightly lower than that reported for other zeolite/polysulfone membranes [33, 34]. The addition of the sodalite particles lowered the membrane selectivity compared to the pure PSF membrane however; the higher porosity SSOD yielded lower ideal selectivity (1.06) than that of the HSOD (1.32). This was attributed to membrane defects and high particle agglomeration of the SSOD. The selectivity displayed by the membranes falls within the range of pure gas selectivity reported in literature (0.083-4.64) [35, 36]. This is encouraging but further studies and mixed gas separations are required to improve on the separation performance of the membranes.

Table 6: Preliminary pure gas permeation results at 1 barg and 298 K

MMM	Pure Gas Permeance ($\times 10^{-9}$ mol/m^2.s.Pa)			Perm-Selectivity		
	H_2	N_2	CO_2	H_2/CO_2	H_2/N_2	N_2/CO_2
PSf	2.73	1.98	1.97	1.38	1.38	1.00
HSOD (5%)	7.31	5.84	5.55	1.32	1.25	1.05
SSOD (5%)	7.60	7.34	7.16	1.06	1.03	1.03

5. Conclusion

Silica sodalite, with enhanced porosity, has been synthesized via topotactic conversion. A 2^3 full factorial design with "a center" was employed to optimize synthesis factors; acid strength, treatment time and calcination temperature. All sodalite samples showed some degree of amorphorization. SSOD 2 displayed the best surface area, pore volume and pore size, which was of the samples produced showed improved surface area and pore volume relative to HSOD. It was assumed that the system was dominated by the main effects and low-order interactions, following the effect sparsity principle [24]. A 1st order regression model was developed utilizing Design Expert v.11, the model produced showed good correlation to the model with a R^2 of 0.716. Calcination temperature was shown to be the only statistically significant model term, decreasing the temperature was found to improve the sodalite pore volume. Acid treatment time was found to have no effect on the response and the effect of acid strength was also insignificant. Optimum parameters were proposed at 1M, 95 minutes and 1073 K. Further study is required to determine optimal variable conditions that yield high quality sodalite with the desired morphology with improved reproducibility. Furthermore, the membranes produced using the porosity-enhanced sodalite displayed comparative H_2/CO_2 separation performance with literature. Further research and development (R&D) is necessary to optimize the synthesis and performance of the membrane in order to produce a competitive membrane-based technology for pre-combustion CO_2 capture.

6. Acknowledgements

CL Eden is grateful to Air Products, South Africa for financial support in this work.

References

[1] C. Scholes, K. Smith, S. Kentish and G. Stevens, "CO2 capture from pre-combustion processes- Strategies for membrane gas separation," *Intarnational Journal of Greenhouse Gas Control,* vol. 4, pp. 739-755, 2010.

[2] D. Jansen, M. Gazzani, G. Manzolini and E. Van Dijk, "Pre-combustion CO2 capture," *International Journal of Greenhouse Gas Control,* vol. 40, pp. 167-187, 2015.

[3] Earth Life Africa Johannesburg, "Climate change, developement and energy problems in SOuth Africa: Another world is possible," OxFam International, Johannesburg, 2009.

[4] K. Lane, IEA Energy Efficiency 2018 and World Energy Outlook 2018, Brussels: International Energy Agency, 2018.

[5] D. Leung, G. Caramanna and M. Mercedes Maroto-Valer, "An overview of current status of carbon dioxide capture and storage technologies," *Renewable and Sustainable Energy Reviews,* vol. 39, pp. 426-443, 2014.

[6] N. M. Anwar, A. Fayyaz, N. F. Sohail, M. F. Khokhar, M. Khokhar, W. D. Khan, K. Rasool, M. Rehan and A. S. Nizami, "CO2 capture and storage: A way forward for sustainable environment," *Journal of Environmental Management,* vol. 226, pp. 131-144, 2018.

[7] [7] Y. Huang, R. W. Baker and L. M. Vane, "Low-Energy Distillation-Membrane Separation Process," *Industrial & Engineering Chemistry Research,* vol. 49, pp. 3760-3768, 2010.

[8] C. Gouedard, D. Picq, F. Launay and P. L. Carrette, "Amine degradation in CO2 capture I. A review," *International journal of greenhouse gas control,* vol. 10, pp. 244-270, 2012.

[9] A. Basu, J. Akhtar, M. Rahman and M. Islam, "A review of separation of gasses using membrane systems," *Petroleum Science and Technology,* vol. 22, p. 1343, 2004.

[10] B. Smith, M. Loganathan and M. Shantha, "A review of the water-gas shift reaction kinetics," *International journal of chemical reactor engineering,* vol. 8, no. Review R4, 2010.

[11] N. Kosinov, J. Gascon, F. Kapteijn and E. Hensen, "Recent developments in zeolite membranes for gas separation," *Journal of membrane science,* vol. 499, pp. 65-79, 2016.

[12] J. Ahn, W.-J. Chung, I. Pinnau and M. D. Guiver, "Polysulfone/silica nanoparticle mixed-matrix membranes for gas separation," *Journal of membrane science,* vol. 314, pp. 123-133, 2008.

[13] M. Daramola, O. Oloye and A. Yaya, "Nanocomposite sodalite/ceramic membrane for pre-combustion CO2 capture: synthesis and morphological characterization," *International journal of coal science & technology,* vol. 4, no. 1, pp. 60-66, 2017.

[14] M. Daramola, A. Dinat and S. Hasrod, "Synthesis and Characterization of Nanocomposite Hydroxy-Sodalite/Ceramic Membrane via Pore-Plugging Hydrothermal Synthesis Technique," *Journal of Membrane and Separation Technology,* vol. 4, pp. 1-7, 2015.

[15] T. Moteki, W. Chaikitisilp, A. Shimojima and T. Okuba, "Silica sodalite without occluded organic maatter by topotactic conversion of lamellar precursor," *American Chemical Society,* vol. 130, pp. 15780-15781, 2008.

[16] K. Momma and F. Izumi, "VESTA 3 for three-dimensional visualization of crystal, volumetric and morphology data," *Journal of applied crystallography,* vol. 44, pp. 1272-1276, 2011.

[17] S. Khajavi, J. Jansen and F. Kapteijn, "Production of ultra pure water by desalination of seawater using a hydroxy sodalite membranes," *Journal of membrane science,* vol. 356, pp. 52-57, 2010.

[18] M. Daramola, B. Silinda, S. Masondo and O. Oluwasina, "Polyethersulphone-sodalite (PES-SOD)Polyethersulphone-sodalite (PES-SOD) mixed-matrix membranes: prospects for acid mine drainage (AMD) treatment," *The South African Institute of Minning and Metallurgy,* vol. 115, pp. 1221-1228, 2015.

[19] T. Moteki, W. Chaikitisilp, Y. Sakamoto, A. Shimojima and T. Okuba, "Role of Acidic Pretreatment of Layered Silicate RUB-15 in its Topotactic Conversion into Pure Silica Sodalite," *Chemistry of materials,* vol. 23, pp. 3564-3570, 2011.

[20] M. Koike, Y. Asakura, M. Sugihara, Y. Kuroda, H. Tsuzura, H. Wada, A. Shimojima and K. Kuroda, "Topotactic conversion of layered silicate RUB-15 to silica sodalite through interlayer condensation in N-methylformamide," *Dalton Transactions,* vol. 46, pp. 10232-10239, 2017.

[21] B. Marler, N. Stroter and H. Gies, "The structure of the new pure silica zeolite RUB-24, Si32O64, obtained by topotactic condensation of the intercalated layer silicate RUB-18," *Microporous and Mesoporous Materials,* vol. 83, pp. 201-211, 2005.

[22] Y. X. Wang, H. Gies and B. Marler, "Synthesis and Crystal Structure of Zeolite RUB-41 Obtained as Calcination Product of a Layered Precursor: a Systematic Approach to a New Synthesis Route," *Chemistry of materials,* vol. 17, no. 1, pp. 43-49, 2005.

[23] R. A. Fischer, The design of experiments, 1st ed., New York: Hafner publishing company, 1935.

[24] D. C. Montgomery, Design and analysis of experiments, 8th ed., Arizona: Wiley and Sons, Inc., 2013.

[25] U. Oberhagemann, P. Bayat, B. Marler, H. Gies and J. Rius, "A Layer Silicate: Synthesis and Structure of the Zeolite Precursor RUB-15 [N(CH3)4]8[Si24O52(OH)4).20H2O," *Angewandte Chemie International Edition in English ,* vol. 35, no. 23, pp. 2869-2872, 1996.

[26] F. Kooli, Y. Liu, K. Hbaieb and R. Al-Faze, "A novel synthetic route to obtain RUB-15 phase by pseudo solid-state conversion," *Microporous and Mesoporous Materials,* vol. 228, pp. 116-122, 2016.

[27] International Zeolite Association, "Database of Zeolite Structures," 2007. [Online]. Available: http://europe.iza-structure.org/IZA-SC/framework.php?STC=SOD.

[28] B. Marler and H. Gies, "Hydrous layer silicates as precursors for zeolites obtained through topotactic condensation: a review," *European Journal of Mineralogy,* vol. 24, pp. 405-428, 2012.

[29] D. D. Reible and F. H. Shair, "A technique for the measurement of gaseous diffusion in porous media," *Journal of soil science,* vol. 33, pp. 165-174, 1982.

[30] T. L. Chitsiga, M. O. Daramola, N. Wagner and J. M. Ngoy, "Parametric effect of adsorption variables on CO2 adsorption of amine-grafted polyaspartamide composite adsorbent during post-combustion CO2 capture: a response surface methodology approach," *International Journal of Oil, Gas and Coal technology,* vol. 17, no. 3, pp. 321-336, 2018.

[31] S. Münzer, J. Caro and P. Behrens, "Preparation and characterization of sodium-free nanocrystalline sodalite," *Microporous and Mesoporous Materials,* vol. 110, pp. 3-10, 2008.

[32] S. Chen, R. Liou, Y. Lin, C. Lai and J. Lai, "Preparation and characterizations of asymmetric sulfonated polysulfone membranes by wet phase inversion method," *European Polymer Journal,* vol. 45, pp. 1293-1301, 2009.

[33] Z. Huang, Y. Li, R. Wen, M. M. Teoh and S. Kulprathipanja, "Enhanced Gas Separation Properties by Using Nanostructured PES-Zeolite 4A Mixed Matrix Membranes," *Journal of applied polymer science,* vol. 101, pp. 3800-3805, 2006.

[34] Y. Li, F. Liang, H. Bux, W. Yang and J. Caro, "Zelitic imidazolate framework ZIF-7 based molecular sieve membrane for hydrogen separation.," *Journal of membrane science,* vol. 354, pp. 48-54, 2010.

[35] P. Jha and J. D. Way, "Carbon dioxide selective mixed-matrix membranes formulation and characterization using rubbery substituted polyphosphazene," *Journal of Membrane Science,* vol. 324, no. 1-2, pp. 151-161, 2008.

[36] E. Karatay, H. Kalıpçılar and L. Yılmaz, "Preparation and performance assessment of binary and ternary PES-SAPO 34-HMA based gas separation membranes," *Journal of membrane science,* vol. 364, no. 1-2, pp. 75-81, 2010.